OFFICE OF NAVAL RESEARCH

Contract No. N00014-91-J-1409

Technical Report No. 145

Some Perspectives on Solution-Phase Electron-Transfer Processes

by

Joseph T. Hupp and Michael J. Weaver

Prepared for Publication

in

Naval Research Reviews

Department of Chemistry

Purdue University

West Lafayette, Indiana 47907-1393

February 1994

Introduction

The kinetics of electron-transfer (ET) processes is a subject graced by a remarkable diversity as well as importance in chemistry and biology. Of the manifold types of chemical ET reactions, those occurring in solution and at electrode-solution interfaces have been the subject of a notably concerted and fruitful research effort. This activity was in large part spawned, and subsequently spurred, by the development of the theoretical treatments by Rudy Marcus and others, now broadly known as "Marcus theory."[1-6] The happy circumstances that enabled the formulation of such quantitative theoretical relationships for solution-phase ET kinetics having true predictive and interpretative value have acted as a considerable impetus to the development of an increasingly diverse and impressive range of experimental activities. These now encompass thermal and photoinduced charge transfers for inorganic, organic, and biological systems in homogeneous solution, ET at metal-solution interfaces, and ET and photo-ET at semiconductor-solution interfaces. Indeed, the ability of the Marcus theoretical framework to interrelate, interpret, and predict ET rates and other dynamical phenomena across such diverse classes of reactions constitutes a major achievement in contemporary physical chemistry, and was undoubtedly responsible in part for the award of the 1992 Nobel Prize in Chemistry to Rudy Marcus.

Along with numerous other experimentalists, our research into electron transfer has been influenced centrally, persistently, and encouragingly not only by Marcus theory, but also by Rudy Marcus himself. In this article we outline some

pertinent issues and experimental inquiries into solution-phase ET phenomena, illustrated in part by findings from our laboratories. Some emphasis is placed on solvent effects, for which the interaction between experiment and theory has been particularly lively and beneficial. For the benefit of the more general reader, we preface this discussion with a short summary of some relevant conceptual and theoretical material. The article also in this issue by Ratner contains further detailed information along these lines.

Some Conceptual Background

The central challenge, met so ably by Marcus theory, is to rationalize, interpret, and predict the seemingly dazzling array of rates observed for solution-phase ET reactions, corresponding to reaction half lives ranging from picoseconds to many months or years! A generalized expression for bimolecular or electrochemical rate constants based on activated-complex theory is[1]

$$k = Z \exp(-\Delta G^{\ddagger}/RT) \qquad (1)$$

where Z is the prefactor and $\Delta G^{\ddagger}$ is the overall free energy of activation. The original Marcus formulations focussed attention on the latter component, understandably so since one expects that the very wide range of observed rate constants can often be attributed primarily to differences in the activation energetics. The framework of Marcus theory provides an extremely useful way in which the various factors which influence $\Delta G^{\ddagger}$ can be separated, identified, and understood.

Particularly useful is the distinction between "intrinsic" and "extrinsic" (or thermodynamic) components, denoting contributions to ΔG^* arising from factors present in the absence, and additional presence, of the free-energy driving force, $\Delta G°$. With the presumption of parabolic free-energy surfaces, the following well-known relation is obtained:[5]

$$\Delta G^* = (\lambda + \Delta G°)^2/4\lambda \qquad (2)$$

In eq. 2, λ is the so-called "reorganization energy", equal to four times the "intrinsic barrier", ΔG^*_{int}, the component of ΔG^* which remains in the absence of a driving force (see Figure 1). Kinetic-based tests of Eq. 2 have attracted much attention, formerly concerning the predicted quadratic log k - $\Delta G°$ dependence in the "normal" driving-force region (where $-\Delta G° < \lambda$)[7], and latterly the *diminishing* rates anticipated with *increasing* driving force in the "inverted" region (where $-\Delta G° > \lambda$) (see below)[8]. While Eq. 2 has limitations under some conditions, the reasonable concordance often observed with experiment, especially in the "normal" free-energy region, is a notable feature of ET phenomena.

Another central aspect of Marcus theory concerns the nature of the intrinsic barrier, ΔG^*_{int}. The Marcus treatment of the outer-shell (solvent) contribution, ΔG^*_{os}, to the intrinsic barrier, based on a nonequilibrium dielectric-continuum model, has proven remarkably resilient; represntative experimental tests based on the energetics of optical ET transitions are discussed below.

Among the more significant consequences of the theoretical treatments

emphasized originally by Marcus, are the interrelationships predicted between rate constants for different outer-sphere reactions featuring common redox couples.[4,5] Probably the best known is a connection between the rate constants for homogeneous-phase cross reactions and for the pair of constituent self-exchange processes. Also significant, however, is the relation predicted between the rate constants for corresponding self-exchange (k^h_{ex}) and electrochemical exchange (k^e_{ex}) reactions:[4]

$$k^e_{ex}/A^e \leq (k^h_{ex}/A^h)^{1/2} \tag{3}$$

where A^e and A^h are the relevant prefactors (*vide infra*). In eq. 3, the extent of the predicted inequality depends on the extent of image stabilization of the electrochemical transition state. Another prediction that has proven useful in mapping reactivity trends in related homogeneous-phase and electrochemical processes is[4]

$$(k^e_1/k^e_2)_E = (k^h_1/k^h_2)_R \tag{4}$$

referring to electrochemical rate constants for a pair of redox couples at a fixed electrode potential, E, in comparison with homogeneous-phase rate constants involving the same pair of couples reacting with a common reagent (oxidant or reductant), R.

It is instructive to consider further the appropriate form of the prefactor terms appearing, for example, in Eqs. 1 and 3. Presumably for simplicity as well as convenience, such terms for outer-sphere ET reactions were initially formulated

on the basis of collision-theory expressions. More recently, it was recognized by Sutin,[9] Marcus,[10] and ourselves[11] that an alternative "encounter preequilibrium" treatment can provide a more useful description of the preexponential factors in both outer- and inner-sphere ET processes.

A general expression for the overall preexponential factor on this basis is[11]

$$A = K_p \kappa_{el} \nu_n \tag{5}$$

where K_p is an equilibrium constant (statistical factor) for forming the precursor state (i.e. with appropriate geometry for ET but prior to nuclear activation). The remaining pair of terms in Eq. 5 refers to the ET activation step itself: the nuclear frequency factor ν_n (s^{-1}) describes the net dynamics of approaching the transition state (associated with nuclear reorganization), and the electronic transmission coefficient κ_{el} denotes the fractional probability with which electron tunneling (so to consummate the reaction) takes place once the transition state is formed. The magnitude of K_p for inner-sphere reactions is clearly governed by the bonding established between the redox centers. For outer-sphere processes, simple statistical expressions can be deduced, depending on the reaction geometry. Thus for homogeneous-phase processes between spherical reactants in the absence of electrostatic work terms:

$$K_p = 4\pi N r^2 \delta r \tag{6}$$

where N is Avogadro's number, r is the reactant separation in the transition state, and δr is a "reaction-zone thickness" denoting the range of internuclear

separations over which electron transfer primarily takes place. A related expression applies to outer-sphere electrochemical reactions, only now $K_p = \delta r$ since the "coreactant" is a planar interface. The values of δr are anticipated typically to be around 1Å, enabling at least approximate estimates of the statistical factor K_p to be obtained.

Another useful outcome of this "encounter preequilibrium" treatment is that it enables the reactivities of related homogeneous-phase and electrochemical processes to be compared in an especially direct fashion.[12] Specifically, the rate constant for a homogeneous reaction involving a pair of redox couples, k_{12}^h, is usefully compared with the electrochemical rate constant involving one of the reactants, k_1°, measured at an electrode potential equal to the formal potential for the coreactant redox couple. In view of Eq. 6, the homogeneous-phase and electrochemical reactivities can be evaluated on a common basis by multiplying the latter by $4\pi Nr^2$. This yields an "equivalent second-order" rate constant, $4\pi Nr^2 k_1 = k_{12}^\circ$, having the same units as k_{12}^h and equalling the electrochemical reactivity in the (hypothetical) circumstance where the electrode "coreactant" offers the same reaction geometry as the homogeneous coreactant. Comparison between the values of k_{12}° and k_{12}^h can provide straightforward insight into the differing environmental factors that influence electrochemical and homogeneous-phase reactivities. This procedure is most useful if the latter rate constants are corrected for the inner-shell (vibrational) activation associated with the homogeneous-phase coreactant. For the resulting k_{cor}^h values, any differences in comparison to k_{12}° values will reflect only differences in the outer-shell (solvent)

reorganization and/or electronic overlap factors between the two reaction environments.

An extensive comparison recently undertaken for inorganic reactions shows that k_{12}° typically exceeds k_{cor}^{b}, the former quantities commonly being as much as 10^2-10^4 fold larger than the latter.[12] Some illustrative rate data of this type are given in Table I. These substantial rate differences, illustrating the often markedly more facile nature of electrochemical outer-sphere processes, most likely reflect the greater efficiency of electron tunneling (i.e. larger κ_{el}) and possibly smaller outer-shell reorganization energy prevalent at metal-solution interfaces.

The physical factors that control the preexponential factor, and especially the nuclear reaction dynamics as reflected in ν_n (Eq. 5), have been the subject of considerable recent interest, particularly with regard to the role of solvation dynamics.[13] In spite of the apparent form of Eq. 5, the nuclear dynamics will only influence the ET rate significantly when the donor-acceptor electronic coupling is sufficiently strong so that $\kappa_{el} \rightarrow 1$ (so-called "adiabatic pathway"). For weaker coupling (such that $\kappa_{el} << 1$) the reaction dynamics will be determined instead by electron tunneling. (In other words, $\kappa_{el}\nu_n$ (= ν_{el}) will be proportional to $(H_{if})^2$, where H_{if} is the electronic coupling matrix element.) Nonetheless, there are many experimental ET systems (including outer-sphere systems), where reaction adiabaticity is achieved (or approached). Consequently, the dynamics of activated nuclear barrier crossing, as denoted by ν_n, should often hold sway over the preexponential factor.

Generally speaking, the overall nuclear frequency factor ν_n will be

determined by the dynamics of both the reactant vibrational (inner-shell) and solvation (outer-shell) components of the activation barrier. In the transition-state theory (TST) limit, ν_n is usually predicted to be governed chiefly by the fastest dynamics (usually reactant vibrations). The role of solvation dynamics, therefore, was originally thought to be unimportant. Recently, however, it has become apparent that significant or even substantial deviations from TST may occur as a consequence of so-called "solvent friction", whereby the dynamics of collective solvent motion (restricted rotations, etc.) required to surmount the ET transition state fall below the dynamics for the rotation of *individual* solvent dipoles (solvent inertial TST limit). Unlike the TST case, the frictional solvent motion is predicted to exert an important or even dominant influence upon ν_n even in the face of considerably more rapid inner-shell dynamics.[14-16] Interestingly, the frictional dynamics can be sensitive to the nature of the solvating medium, so that distinctly different solvent-dependent ET kinetics are anticipated depending on whether the activation energetics, or additionally the solvent dynamics, influences the reaction rate.[13] This issue is considered further below.

Solvent Barriers

One of the earliest features of the theoretical treatments now collectively known as "Marcus theory" was a unique description of condensed-phase ET activation barriers as nonequilibrium solvent polarization barriers.[1-5] A schematic representation of the barrier effect is shown below. A more quantitative

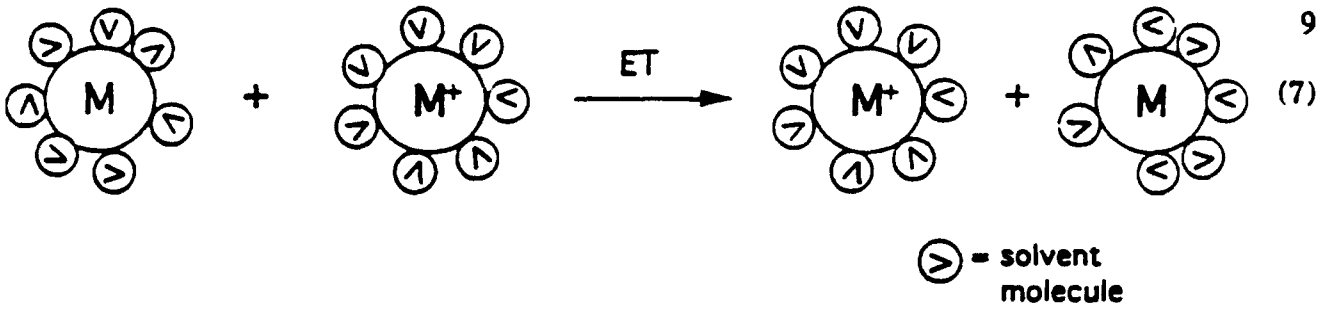

(7)

representation followed from the recognition by Marcus that a transferring charge (electron) would essentially instantaneously perturb the bound electrons associated with the surrounding medium (i.e. polar solvent), but would only slowly (in comparison to the timescale for an electronic transition) perturb the solvent nuclei. The relatively slow nuclear response was expected to create an intrinsic barrier to ET that could be surmounted by random solvent polarization fluctuations. The barrier was theoretically characterized, therefore, by both high frequency (ε_{op}) and low frequency (ε_s) dielectric components (corresponding to fast (electronic) and slow (nuclear) polarization responses). Further consideration of the electrostatic consequences of finite molecular reactant size (radius, r) and finite reactant separation distance or image distance (d) led to the following barrier expressions:

$$\Delta G^* = (e^2/4)\{(1/2r_1) + (1/2r_2) - 1/d)\}\ (1/\varepsilon_{op} - 1/\varepsilon_s) \qquad (8a)$$

$$\Delta G^* = (e^2/8)(1/r - 1/d)(1/\varepsilon_{op} - 1/\varepsilon_s) \qquad (8b)$$

where Eq. 8a is applicable to homogeneous solution-phase reactions, Eq. 8b to interfacial electrochemical processes, and e in both equations is the unit electronic

charge. As suggested by Eq. 8, the polarization analysis offers some remarkably simple predictions as to how barriers and, therefore rates, for electron transfer should depend on macroscopic solvent properties, as well as molecular reactant size and geometry. Nevertheless, compelling experimental evidence in support of the solvent barrier theory was lacking for a number of years, despite several seemingly straightforward kinetics investigations, (such as rate studies as a function of the solvent, etc). In retrospect, many of these studies were bound to fail in this context because of the existence of other important solvent-variable kinetic factors, most notably: 1) electrostatic work terms (including interfacial adsorption and solution-phase ion pairing), and 2) dynamics effects (see below). In addition, at least some of the systems chosen for evaluation at *electrochemical* interfaces (for example, reduction of protons to dihydrogen) were inappropriate because they involved extensive bond creation or annihilation.

Given these circumstances, a key experimental development was the design and synthesis (largely by the Meyer[17,18] and Taube[19,20] groups) of molecular donor-acceptor (D-A) systems featuring well-resolved charge-transfer absorption bands.[21,22] When these systems are symmetrical (i.e. when the donor and acceptor sites are chemically identical as in Eq. 9), the absorption energy (E_{op})

$$(bpy)_2ClRu^{II}-bridge-Ru^{III}Cl(bpy)_2^{3+} \xrightarrow{h\nu} (bpy)_2ClRu^{III}-bridge-Ru^{II}Cl(bpy)_2^{3+} \quad (9)$$

(bpy = 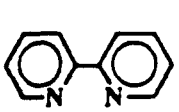 bridge = 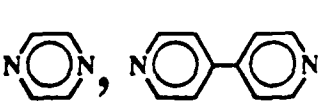 or 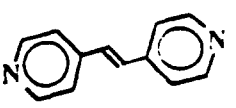)

for the lowest charge-transfer transition can be identified directly with the (vertical) Marcus reorganization energy, λ.[23,24] As already noted (Fig. 1), the reorganizational parameter, in turn, can easily be related to the expected thermal ET activation energy, $\Delta G^{\ddagger}$. For parabolic energy surfaces (i.e. those derived from displacement of harmonic oscillators) the energy relationship is simply:

$$\Delta G^{\ddagger} = \lambda/4 \; (= E_{op}/4) \tag{10}$$

Shortly after the appearance of the first valence-localized D-A studies,[18,21] systematic variations in bridge length were examined,[17] leading to a verification of the predicted dependence (Eq. 8a) of the solvent reorganization energy on D-A separation distance d (Fig. 2).

A central aspect of the optical ET strategy — as exemplified by the system illustrated in Fig. 3 (Eq. 11) is the evaluation of the reorganization energy (or

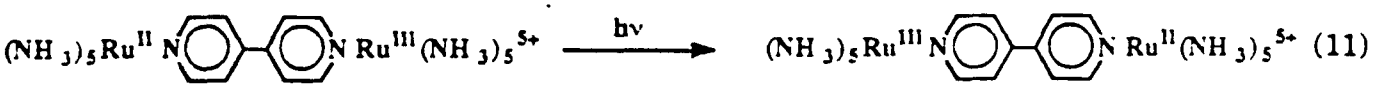

(11)

optical ET barrier) as a function of the solvent dielectric properties. The dependence found in this example,[25,26] and in several others, clearly is consistent with the qualitative predictions of the polarization theory (Eq. 8). We — along with the Brookhaven group[27] — have noted, however, that quantitative agreement is lacking: the extent of variation of λ with solvent is (in this instance)

markedly *less* than anticipated from theory. A clue to the origin of this disparate behavior is provided by the ET distance-dependent study in Fig. 2. The normal charge-transfer distance in reaction 11 (i.e. the ruthenium-to-ruthenium distance) is 11.3 Å. The detailed chemistry, however, is such that the pertinent $d\pi$ metal orbitals mix (selectively) with bridging ligand orbitals of the same symmetry (both π and π^*) and become significantly polarized along the charge-transfer axis. The effective ET distance, as recently determined by electronic Stark-effect spectroscopy,[28] is closer to 6Å. A shorter charge-transfer distance should lead to correspondingly less polarization of solvent and smaller reorganization energies (again, note Fig. 2). With the experimentally determined distance modification, we find that agreement with the dielectric-continuum theory now becomes essentially quantitative.[25]

Related work on the solvent barrier/ET reactivity problem - in this case by the Brookhaven group[29] — has revealed the spectacular consequences of simple variations in molecular size. This group showed, for example, that systematically increasing the average molecular radii of pairs of simple transition-metal complexes (from 7 Å to 14 Å) could increase bimolecular (homogeneous) electron-exchange rates (Eq. 12) by over five orders of magnitude![29] The observed

$$M(L)_x^{3+} + M(L)_x^{2+} \rightleftharpoons M(L)_x^{2+} + M(L)_x^{3+} \qquad (12)$$

reactivity variations are almost undoubtedly solvational in origin, as the redox pairs were carefully chosen so as to minimize reactant vibrational barriers (see below) as well as nonadiabaticity (κ_{el}) effects. Interpretation of the experiments in

terms of nonequilibrium solvent-polarization phenomena provides a quantitative explanation for the reactivity pattern once the secondary influence of reactant size on separation distance (d; Eq. 2) is also taken into account. From a primitive physical perspective, the size dependence arises, then, from two sources: 1) a diminution of the effective charge density on the surfaces of the reacting molecular spheres (and therefore a decrease in surrounding solvent polarization) with increasing sphere size, and 2) a diminution of partially compensating image-charge interactions as the center-to-center distance (d) for each reacting pair is likewise increased.

Surprisingly, only recently have the corresponding effects of reactant size on electrochemical reactivity been explored. As Figure 4 illustrates, rates for

$$M(L)_x^{3+} + e^-(\text{electrode}) \rightleftharpoons M(L)_x^{2+} \qquad (13)$$

interfacial ET (Eq. 13) have been observed to increase exponentially with decreasing effective reactant radius.[30] This observation is broadly consistent, of course, with a Marcus-type solvent barrier effect. Two additional points, however, are worth noting. First, the magnitude of the kinetic size effect (spanning roughly two orders of magnitude in ET rate, and corresponding to ca. 3 kcal mol^{-1} in barrier height) is considerably less than found in the study of homogeneous bimolecular reactivity noted above. The most important difference chemically between the two studies is the involvement of only a single molecular reactant in each of the electrochemical processes, versus two reactants in the solution-phase processes. At a crude intuitive level one would expect, therefore, roughly half the

extent of solvent repolarization in the former as the latter. Indeed, this notion — expressed more rigorously by Marcus[2-5] — underlies the so-called homogeneous/heterogeneous cross relationship (see Eq. 3) that permits solution-phase reactivities to be predicted from electrochemical kinetics data and vice versa. The second point is that two of the reactants in the electrochemical study are actually small diameter reactants whose effective sizes have been increased by covalently linking them to an additional reactant and then delocalizing the associated charges over the resulting "super molecule". We suggest that this could prove to be a more generally effective strategy for accelerating outer-sphere electron-transfer reactivity. In any case, it provides a simple illustration of the experimental exploitation of basic barrier concepts to manipulate reactivity.

As perhaps suggested by the preceding discussion, one of the active areas of current research is the synthetic manipulation of specific chemical systems to provide detailed control of solvent-based barrier effects. Several reports from Curtis and co-workers have illustrated how control can be exerted via a clever combination of mixed solvation and selective reactant/solvent hydrogen bond formation.[31,32] Related studies at Northwestern have illustrated how local solvation can be manipulated to: a) trigger kinetically observable intramolecular ET events,[33] b) create barriers and induce valence localization (or partial localization) in otherwise delocalized, multi-site systems,[34] and c) significantly modulate superexchange-based electronic coupling effects.[35]

Another important focus of contemporary research is solvent "molecularity". The nonequilibrium solvent polarization theory of Marcus achieves its simplicity

and broad applicability, in part, by representing the solvent as a structureless, polarizable medium, i.e. "molecularity" is intentionally neglected. Nevertheless, molecules — including solvent molecules — are obviously of intrinsic interest to chemists! Recent attempts to gain a more molecular-level understanding of solvent reorganization effects have proceeded along at least four different lines. One involves the introduction of a mean spherical approximation (MSA) for individual solvent molecules, within the context of a broader electrostatic representation of medium repolarization effects. An interesting MSA-based model due to Wolynes treated the nonequilibrium solvation problem in terms of a frequency-dependent Gurney cosphere engendered by the solvent molecular size.[36] This approach, along with other MSA treatments, usually yields reorganization energies that are somewhat (say 15-25%) smaller than obtained from the conventional continuum estimates. A numerical comparison with solvent-dependent E_{op} values for biferrocene species indicates a rough concordance in several aprotic solvents, although not in hydrogen-bound media.[37] A more recent MSA treatment by Blum and Fawcett for equilibrium solvation (i.e. the zero-frequency part of the solvent reorganization energy) emphasizes anticipated differences between the solvation of cations and anions.[38] This model has also been applied to an analysis of the solvent-dependent electrode kinetics of $Cp_2Co^{+/0}$ versus $Cp_2Co^{0/-}$ (Cp = cyclopentadienyl).[39] Interestingly, the MSA model can account for the observed more sluggish kinetics of the latter couple, from the predicted higher solvent activation barrier, although other factors (inner-shell barriers, specific double-layer effects, ion-pairing, solvation dynamics, etc.) perhaps

also play a role. The evaluation of E_{op} data for differently charged mixed-valence systems in this context would be worthwhile.

An alternative, perhaps complementary, semi-emperical approach to estimating $\Delta G^{\ddagger}$ is the so-called "nonlocal" electronic treatment due to Kornyshev and Ulstrup,[40] which considers the effects of spatial correlation on the wavevector-dependent solvent dielectric properties. One worthwhile facet of this model is that it can provide a viable rationalization of some deviations from the continuum predictions observed for metallocenes in hydrogen-bound media.[37,41]

A second, fundamentally different, approach to molecular solvent reorganization makes use of molecular-dynamics (MD) simulations and carefully chosen potentials for solvent interactions. Some encouraging results based on this strategy have emerged from Chandler and coworkers[42] (see also the article in this issue by G. Voth). This group has successfully simulated the redox activation behavior of the well-known hexaaquo iron(III/II) system in water as solvent, and has derived important new insights regarding the role of nuclear tunneling.[42] Most notably, they found a remarkable concordance with the Marcus prediction of parabolic potential-energy surfaces for solvent reorganization, even though complex short-range interactions abound in this highly charged/hydrogen-bonded system. On the other hand, model MD simulations for both dipole creation/annihilation[43] and ET[44] in methanol show clear evidence for non-linear polarization effects, that is, significant deviations from parabolic free-energy surfaces. The latter simulations also yield higher activation barriers for anion-neutral than for cation-neutral reactant pairs (*vide supra*) attributable to short-

range solvation, although the effect is small for reactant radii approaching those prevalent in ET phenomena.[44] Overall, while such MD simulations can be complex and time consuming, they are beginning to add a new molecular-level dimension to our understanding of the energetics of nonequilibrium solvation. The associated dynamical aspects are discussed briefly below.

A third approach is largely experimental and focuses on the controlled assembly of orientationally constrained, local solvent environments (for example, large "encapsulating" crown ethers, semi-rigid hemicarcerands, etc.). Such assemblies may be amenable to detailed *in situ* (multidimensional NMR) and/or *ex situ* (crystallographic) structural characterization as a function of encapsulated reactant or product oxidation state. Initial studies have shown that the overall solvent reorganizational energetics for such systems can readily be monitored by optical ET methods (cf. Eq. 12).[45] Finally, a fourth approach – pioneered by Hendrickson and co-workers – involves solid-state electron transfer.[46] Single crystals of various molecular mixed-valency species are prepared with zero, one, or two solvent molecules of co-crystallization. Coupling of isolated solvent motions to ET can then be examined via a combination of X-ray and variable-temperature Mossbaur spectroscopy techniques.

The presence of such a myriad of molecular solvent reorganization treatments notwithstanding, it is worth reiterating that the Marcus dielectric-continuum approach remains a generally useful, and in most cases, a semiquantitatively (or even quantitatively) reliable means of estimating total ET solvent reorganization energies. That this should be the case even though the

relevant physics contains a common element with the Born solvation model — well known to be much less reliable — lies partly in the usual dominance (at least in polar media) of the optical frequency component (ε_{op}^{-1}) with respect to the Born term (ε_s^{-1}) in Eq. 8. Indeed, quite marked deviations between the equilibrium solvation energies and the Born predictions can occur without influencing substantially the *nonequilibrium* solvation energy (λ or ΔG^*). We discussed this point some time ago in an analysis that harnesses experimental solvation energies for redox couples (i.e. differential solvation energies) in place of the Born term in Eq. 8.[47]

Other solvent related issues of current interest and importance include: 1) "solvent" reorganization in protein environments (where again, additional molecular-level theory development would be invaluable), 2) solvent reorganization at *non*metal/solution interfaces — for example, liquid/liquid interfaces, semiconductor/solution interfaces, and membrane/solution interfaces, and 3) solvent reorganization at mesoscopic and nanoscopic particle(or electrode)/solution interfaces. Some insightful theoretical work on liquid/liquid and semiconductor/liquid interfaces has appeared recently from Marcus[48] and from Smith and Koval.[49] Experiments capable of testing these theories would be most useful. Finally, in the mesoscopic chemistry field, a number of exciting experimental developments relating to interfacial ET and energy conversion have emerged in the last three years, in particular.[50-52] Fundamental studies of barrier phenomena here could provide a rational basis for further advances and could help to explain some of the more provocative existing results.

Vibrational Barriers

A second major component of most ET reaction barriers is vibrational reorganization. This component arises because of the oxidation-state dependence of the normal coordinates or internal bond lengths. Interconversion of oxidation states (electron transfer) therefore requires the displacement of coordinates (bond compression or bond stretching) and is accomplished, in the Marcus classical limit, by vibrational activation.[3,5,53] The combination of net coordinate displacement and transient vibrational excitation leads to an energy barrier shaped much like the one in Figure 1. In this picture, the actual charge transfer occurs at the top of the barrier (the transition state) where the best compromise, in terms of bond lengths, has been achieved between the redox reactant and product. According to Marcus, the vibrational activation barrier (ΔG^{*}_{vib}) or reorganization energy (λ_{vib}) for an electron exchange reaction (homogeneous or electrochemical) can be estimated simply from known bond length changes (Δa) and associated force constants (f):

$$\Delta G^{*}_{vib} = \tfrac{1}{8} \sum_{j} b(\Delta a_j)^2 f_j \qquad (14)$$

In Eq. 14, b is the number of equivalent bonds displaced, and the summation (j) is over all bonds displaced.

The importance of vibrational reorganizational effects can hardly be overstated. For example, Brunschwig et al,[54] in a study of about a dozen transition-metal redox couples, found that bimolecular self-exchange rate

variations over some *15 orders of magnitude* could be explained almost entirely on the basis of classical vibrational activation effects. We showed in a related study that similar effects can also control reactivity for cross reactions and at electrochemical interfaces.[55] Figure 5, for example, shows a plot of standard double-layer corrected electrochemical rate constants for four transition-metal complexes of similar size versus independently estimated vibrational activation energies. As in the Brunschwig study, a reasonable correlation exists.

In both the examples above, vibrational barriers were derived from X-ray measurements (EXAFS or crystallography) of metal-ligand bond lengths in oxidized and reduced states, with the bond length differences then incorporated into Eq. 14. This strategy is useful when: a) normal coordinate displacements can be approximated by local coordinate (i.e. bond length) displacements, b) the number of coordinates or types of bonds displaced is small, c) both redox states are chemically stable and long lived, and d) the available crystalline or solution X-ray measurement environment is sufficiently similar to the redox reaction environment to yield kinetically meaningful structural data. In many cases, however, one or more of these conditions is not fulfilled, and alternative routes to structural data are required. Viable routes include: 1) Franck-Condon analysis of structured emission (fluorescence or phosphorescence) from photo excited electronic states,[56] 2) empirical correlations (e.g. Badger's rules, etc.) of redox-induced vibrational frequency shifts with normal or local coordinate displacements,[57] and 3) time-dependent analysis of resonance Raman scattering intensities.[58]

Over the past few years the Northwestern group[59-62], and the Myers group at Rochester,[63] have made extensive use of the third strategy and have found it to be extremely powerful. To implement the strategy, it is necessary to identify electronic absorption bands corresponding to the thermal electron transfer reaction of interest. This is reasonably straightforward for homogeneous solution-phase reactions. We find, however,[61] that the Raman method can also be applied to interfacial reactions such as reaction 15:

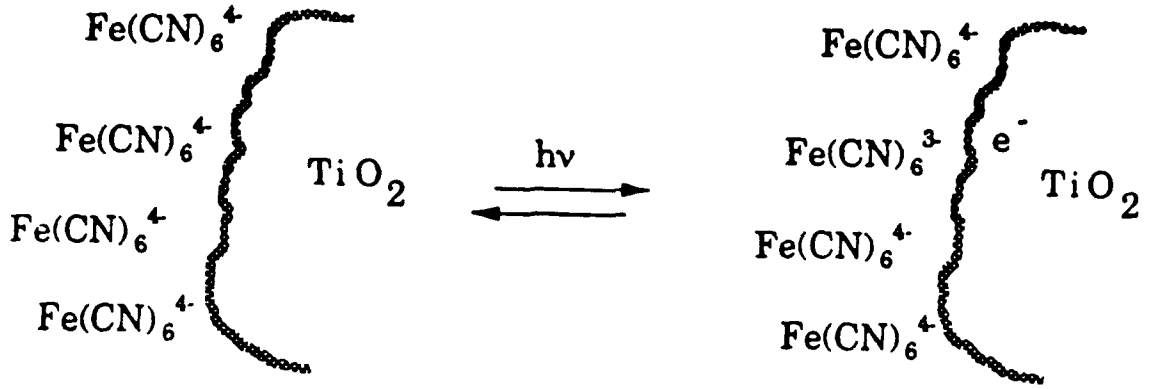

(15)

Visible region excitation of an intense ferrocyanide to titanium dioxide (particle or electrode) charge transfer band leads, in this case, to enhanced Raman scattering from nearly a dozen vibrational modes. Observation of enhancement implies vibronic coupling of these modes to the transition of interest, i.e. Eq. 15 or the reverse. Time-dependent theory then permits one to connect the observed scattering intensities quantitatively to normal coordinate displacements (Δ) — which, in turn, may be transformed into bond length changes. Table II summarizes the results of such an experiment. A number of points are worth noting. First, the symmetry of the molecular system is clearly reduced by surface

binding, resulting in activation of several vibrational modes which are completely undetectable in solution or single crystal environments(i.e. X-ray measurement environments). Second, the electrode (i.e. TiO_2) lattice itself is activated by interfacial ET. Third, the overall vibrational barrier can be partitioned into high- and low-frequency components. This then permits important tunneling corrections to the classical Marcus vibrational analysis to be applied in a mode-specific fashion. Finally it is worth noting that this particular system would be very difficult to examine by conventional structural methods because the redox form on the right hand side of Eq. 15 returns to the initial form in less than 400 ns.[64] The Raman method overcomes this problem by interacting with the short-lived state only in a resonance fashion; significant real lifetimes, therefore, are not required.

It is appropriate to conclude this section by outlining some of the current issues and problems in this area of redox chemistry. One of these concerns bridged systems where coupling of bridge-localized vibrations to intramolecular ET is of appreciable theoretical, as well as experimental, interest. Also currently being investigated — primarily by resonance Raman in the extended near infrared — is the question of how specific vibrational modes conspire to cause electronic localization versus delocalization in more strongly electronically coupled systems.[65] Conceptually related to the Raman studies, and especially the time-dependent scattering studies, are new theoretical studies involving wave packet propagation methods. These studies, being carried out primarily by Nitzan and Ratner[66] (see accompanying article), may offer significant insights into the real-

time progress of ultrafast ET reactions. The increasing *experimental* availability of ultrafast techniques (i.e. laser-based techniques which can probe reactions in the 15 to 50 femtosecond time regime) should soon permit some very exciting issues in rapid-reaction chemistry to be examined. One of these concerns coherence effects, where extremely fast reverse ET might, in fact, provide a fundamental dephasing mechanism for rapidly created states. On a slightly longer timescale (i.e. 0.5 to 5 picoseconds) the availability of tunable transient infrared spectrometers may permit one to understand how ET product states dispose of excess vibrational energy and reconfigure themselves for further reaction. Indeed, preliminary studies along these lines (by Doorn, Dyer, Woodruff and Stoutland at Los Alamos[67]) appear promising. Transient IR methods should also permit chemists to examine how photochemically generated, vibrationally hot systems behave in redox transformations. This problem could be of particular importance in molecule-based studies of solar energy conversion. Emerging work from Spears and co-workers[68] suggests that highly unusual reactivity patterns will be seen. Other solution-phase work of interest concerns reactions where the formation of one or more bonds directly accompanies the transfer of a single electron. A specific example, from the Barbara group, involves charge transfer between a halogen atom and a dimeric (van der Waals) benzene cation.[69] Here two bonds appear to be formed. Interestingly, adequate understanding of the problem — in both a dynamic and a vibronic sense — would appear to lie beyond the realm of current theory.

Returning to surfaces or interfaces, the unexpected observation of electrode

lattice activation during electron transfer (Eq. 15) merits further investigation. Is the phenomenon restricted to semiconductor materials, or might it also be significant at metal surfaces? For either class of material or surface, are there vibrational activation consequences for quantum confinement, i.e. for geometrically constraining the transferred electron or hole within an electrode or particle of smaller size than the characteristic e^- or h^+ radius? Both questions could be of importance in emerging redox-based applications of colloidal particle dispersions. We further suggest that both may be amenable to investigation by systematic electrochemical, spectral and theoretical studies of cluster systems. Finally, one may ask whether there are likely to be unusual local, or collective, vibrational effects in reactions involving self-assembled monolayers. Preliminary studies by Abruna and co-workers, based on an unusual X-ray standing wave method, indicate that there are.[70] In the X-ray study clear evidence is found for coupling of an "accordion" type bridge compression motion to ET between an electrode and a tethered transition-metal reactant. Also of interest is a very recent observation by Bedzyk and Mirkin of long range two-dimensional ordering in a redox-active monolayer (again via standing-wave techniques).[71] These new experiments should open up the possibility of detecting and evaluating collective coordinate displacement effects in interfacial ET processes. Interestingly, collective — or at least correlated — coordinate displacements appear to play a *very* important role in the kinetics of ET in solid-state environments (i.e. three-dimensional crystalline environments), as demonstrated by Hendrickson and co-workers.[46]

Driving Force Effects

Just as important (in a kinetic sense) as solvational and vibrational reorganization energies are the effects of thermodynamic driving forces (reaction free energies). As suggested by eqs. 1 and 2, the way in which driving forces affect ET rates is primarily through classical barrier height manipulation (although other effects, such as electronic tuning, are known). For small changes in driving force (ΔG°) a linear variation in ΔG^* is predicted by Marcus theory; for larger changes the expected variation is quadratic. In other words, an exponential, or nearly exponential, increase in ET rate with increasingly favorable driving force is predicted — much as in other transition-state theories. A very large number of examples of this type of behavior have been described experimentally.

More unusual is the prediction, already noted, that for very large driving forces ($-\Delta G^\circ > \lambda$), electron-transfer rates should *decrease* with increasing exoergicity, i.e. "inverted" rate versus driving force behavior should be seen. This well-known prediction proved quite resistant to verification, leading many to conclude that the underlying theory was not fully correct. In 1979, however, inverted rate behavior — consistent with Marcus theory — was finally observed by Beitz and Miller for a series of bimolecular ET reactions in low-temperature glasses.[72] Nevertheless, because of the exotic medium, many researchers were skeptical. Ultimately, in 1984 — nearly 30 years after the initial theoretical proposal — Miller, Calcaterra, and Closs provided an even more convincing demonstration of rate inversion.[73] These experiments involved intramolecular ET

and were based on a clever application of pulsed radiolysis methods to solution-phase kinetics. In retrospect, the functional equivalent of inverted ET was, in fact, seen some time before in various studies of nonradiative decay with organic[74] (and later inorganic[75]) chromophores — as both Marcus[76] and Meyer[77] have noted. It is now generally appreciated that the so-called "energy-gap law", often used to characterize these experiments, can be obtained from a low-temperature quantum version of Marcus' classical inverted-region analysis.

Since 1984, more than two dozen additional examples have appeared, encompassing a variety of chemical contexts. For illustrative purposes we will focus on two of the more recent. The first is represented schematically by the photo-redox sequence shown below (where Ir_2 is [Ir(1,5-cyclooctadiene)(μ-pyrazolyl)]$_2$ and py^+ is any of several alkyl pyridinium ions):[78]

$$Ir_2 \xrightarrow{h\nu} Ir_2^* \qquad (16a)$$

$$Ir_2^* + py^+ \xrightarrow{h\nu} Ir_2^{\bullet+} + py^\bullet \qquad (16b)$$

$$Ir_2^{\bullet+} + py^\bullet \xrightarrow{h\nu} Ir_2 + py^+ \qquad (16c)$$

Note that ET is bimolecular and that it can occur in two directions. Furthermore, Gray and co-workers have shown that the driving force can be made to exceed λ in both.[78] Surprisingly, however, rate inversion occurs only in the reverse direction (i.e. diiridium cation reduction, eq. 16c). In the forward direction, rates increase to a diffusion-limited value with increasing $-\Delta G^\circ$, but are then unresponsive to further increases in driving force. Several explanations have been devised. But,

as yet, none have been confirmed. The second example is shown in Figure 6 and comes from Northwestern.[64] The reaction involved is Eq. 6, where the driving force has been varied by replacing one of the six available CN^- ligands of the parent compound with any one of several pyridyl ligands. The absolute driving forces are unknown at present, but clearly they will scale as the formal potentials (E_f) of the molecular reactants in solution. In this case it also has been possible to calculate the slope of the rate vs. driving-force plot by using Raman-derived displacement and force-constant data (Table I) and low-temperature theory. The calculated slope (roughly a factor of ten decrease in rate for a 300 mV increase in driving force) is in good agreement with experiment. Perhaps surprisingly, the experiment represents the first in which rate inversion has been observed at an interface.

Among other important current issues and problems relating to driving-force phenomena are: 1) "gating" effects (see article by Ratner) which may decouple ET from very slow nuclear coordinates and make certain ET processes driving-force independent,[79-82] 2) exploitation of rate inversion to inhibit reverse ET — and enhance efficiency — in artificial, molecule-based solar energy conversion devices,[83] and 3) adaptation of Marcus-type analyses to atom and ion transfer reactions.[84,85]

Reaction Dynamics

We have so far focussed attention primarily on the energetic aspects of ET chemistry, that is the factors and strategies utilized to understand and evaluate

energy barriers. A complete description of ET kinetics, however, also necessarily involves evaluation of the reaction dynamics, that is, the rapidity by which the system is able to move along the reaction coordinate so to yield products from reactants. As already noted, several factors may influence the reaction dynamics, and hence the preexponential factor for activated ET processes, not the least of which is the electron-tunneling probability for nonadiabatic processes. Much experimental information on the kinetic consequences of electronic coupling in nonadiabatic ET has been gained from intramolecular D-A systems where the donor and acceptor sites are separated by extended and/or saturated organic linkages. These include deliberately synthesized systems,[73,86] as well as modified biological systems such as metalloproteins,[87] both of which also have been featured prominently in tests of driving-force effects (see above). In the context of electronic coupling effects, primary tactics involve discerning the kinetic response to alterations in the spatial and/or structural D-A separation. Besides homogeneous-phase intramolecular ET, substantial advances have been made along these lines for structurally well-defined films at electrochemical surfaces.[88,89]

We confine our comments here primarily to the reaction dynamics anticipated for adiabatic processes, where nuclear (especially solvational) rather than electronic factors should prevail. Up to the late 1970's, theoretical treatments of solvent effects, including Marcus theory, focussed on activation energetic aspects. Beginning around 1980, and continuing to the present, substantial research effort has been invested in understanding the *dynamical*

roles of reactant solvation.[91-99] Progress has been driven, in particular, by the recognition of "solvent-friction" effects in chemical kinetics (which, as mentioned above, constitute an interesting deviation from the usual TST approach). While the precise physical meaning and interpretation of solvent-friction effects depend somewhat on the type of reaction being considered, the usual notion is that an impediment exists to net progress along the reaction coordinate, because of irreversible energy dissipation from the "reactive" (possibly solvent molecular rotation) modes to the surrounding solvent "bath". The reaction coordinate motion is then no longer smooth and unidirectional (as in TST) but is characterized instead by "fits and starts", commonly termed "overdamped motion", perhaps even involving several recrossings within the barrier-top region before the reaction is finally consummated.

While ET was historically not the first class of reactions for which the notion of solvent friction was considered in dynamical descriptions, the central role of solvation in the ET reaction coordinate attracted attention in this context by theoreticians by the early 1980's.[91-93] Since then, the literature has theoretical has expanded enormously. Most of this work emphasizes the idea that "dielectric friction", associated physically with collective rotations (and related motions) of solvent dipoles that necessary attend solution ET processes, should exert significant or even substantial influences upon the net barrier-crossing dynamics, and hence the ET reaction rate.

The emergence of this theoretical framework has inspired a large number of experimental studies aimed variously at probing the nature of, and the extent to

which, collective solvent polarization can influence the dynamics of ET and related processes. Broadly speaking, the experimental inquiries fall into four categories. The first (type I) involves the evaluation of time-dependent fluorescence Stokes shifts (TDFS) for solute chromophores forming suitable charge-transfer excited states.[100,101] In optimal cases, these ultrafast ($\gtrsim$ 50 ps) laser-induced measurements can probe directly the real-time dynamics of polar solvent relaxation around a newly formed solute dipole, and have yielded some fascinating information of relevance to ET kinetics. The second type concerns a related use of ultrafast pulse lasers to follow intramolecular ET processes emanating from phototexcited states.[101] So far, however, almost all of the ET reactions studies in this fashion involve only small free-energy barriers, $\Delta G^{\ddagger} \lesssim k_B T$ (k_B is Boltzmann's constant).[101,102] (The additional role of *inertial* solvent motions, therefore, can probably not be overlooked.)

The remaining two experimental categories constitute attempts to extract information concerning dynamical solvent effects for *activated* ET processes (say, for $\Delta G^{\ddagger} \gtrsim 5k_B T$). The most common approach (type III) involves the acquisition of solvent-dependent kinetic data for bimolecular outer-sphere electron-exchange reactions, especially symmetrical self-exchange, and for related reactions at electrode surfaces.[13] The kinetics of the former are most commonly evaluated by means of magnetic resonance (nmr, epr) line-broadening methods. These reaction systems feature significant (commonly 5-10 $k_B T$) solvent reorganization barriers (i.e., they truly are activated processes). In addition, these systems provide opportunities to examine the dynamical consequences of systematically altering

solute-solvent interactions, reactant electronic structure, vibrational barriers, etc. Despite the clear fundamental importance of activated ET processes, however, the experimental extraction of information on barrier-crossing dynamics is somewhat problematic. The core of the problem concerns the need to separate the dynamical (preexponential factor) and energetic (barrier height, $\Delta G^{\ddagger}$) contributions to the measured solvent-dependent rate constants. In most cases, the extraction of the desired dynamical information from rate data requires one to use theoretical estimates for $\Delta G^{\ddagger}$. An additional problem in these conventional analyses is that the geometry as well as stability of the precursor complexes for bimolecular (or electrochemical) outer-sphere processes is often unknown.

The conclusions regarding the role of solvent dynamics reached in this fashion are therefore often critically dependent on the validity of the theoretical models utilized to separate the dynamical and energetic factors. These type III tactics have consequently tended to be regarded as a "poor cousin" in comparison with the more direct (and sophisticated-looking) insight into real-time dynamics obtained from approaches I and II. Most of the uncertainties faced with such dynamical analyses for activated ET reactions could be circumvented by evaluating solvent-dependent rate data for intramolecular (preferably symmetric) ET reactions (labelled here as type IV). The evaluation of both the unimolecular ET rates and the barrier heights (the latter from optical ET energies) would provide the preferred route to the separation of dynamical and energetic factors. Unfortunately, however, relatively few type IV systems have been scrutinized in the context of solvent dynamics.[103]

Despite the complications, sufficient information on barrier height and related factors can be obtained for certain *bimolecular* ET reactions to allow reliable, and even quantitative, deductions to be made regarding solvent-dependent barrier-crossing dynamics. The specifics have been reviewed in some detail recently.[13,102] Broadly speaking, the extant experimental information lends support to the earlier theoretical predictions that overdamped solvent motion ("solvent friction") can often influence and even control the ET barrier-crossing dynamics, as prescribed most simply by the longitudinal solvent relaxation time, τ_L. While a large number of type III reactions (both homogeneous and electrochemical) have now been examined, one series of systems studied by the Purdue group a few years ago provides an interesting example of what may be discerned experimentally in optimal cases. The series consists of metallocenium-metallocene self-exchanges:

$$Cp_2M^+ + Cp_2M = Cp_2M + Cp_2M^+ \qquad (17)$$

where Cp is a cyclopentadienyl ligand (or derivative), and M is iron or cobalt.[13,104-107] The reactions were selected for several reasons, including the dominance of outer-shell (solvent) reorganization in the activation energetics, and the opportunity to modulate the relevant electronic properties via both metal and ligand alterations.

Figure 7 shows a logarithmic plot of the self-exchange rate constant k_{ex} ($M^{-1}s^{-1}$) for five metallocene couples versus the inverse longitudinal relaxation time for a range of solvents (see caption and ref. 107 for details). The rate constants k_{ex}

were corrected in an approximate way for solvent-induced variations in barrier height via comparisons to optical ET data for a related mixed-valence ferrocenium-ferrocene system; solvent-induced variations in k_{ex} for a pair of given self-exchange reactions, therefore, should reflect only differences in the reaction dynamics (i.e. $\kappa_{el}\nu_n$ in Eq. 5). The τ_L^{-1} parameter, extracted from dielectric loss spectra, provides an approximate assay of the overdamped solvent dynamics in so-called "Debye" media (those characterized by only a single relaxation time). While the solvents selected for Fig. 7 generally exhibit only approximate Debye behavior, the solvent friction dynamics (i.e. the τ_L^{-1} values) are seen to span a substantial numerical range (ca. 1×10^{11} s^{-1} to 4×10^{12} s^{-1}).

Interestingly, the sensitivity of the ET rates to the solvation dynamics varies systematically with the nature of the metallocene: The slowest reactions (ferrocenium/ferrocene) are insensitive to the solvent dynamics, while the fastest (cobaltocenium/cobaltocene) vary almost proportionally with τ_L^{-1} — with intermediate behavior seen for others. This spectrum of reactivity can be rationalized on the basis of a transition from nonadiabatic to adiabatic behavior (see Background section above). The slowest reactions follow largely nonadiabatic ET pathways, so that the barrier-crossing probability is essentially proportional to $(H_{if})^2$ and *independent* of the solvation dynamics. For reactions featuring larger D-A electronic coupling (larger H_{if}), reaction adiabaticity is approached or reached, and the reaction dynamics become highly sensitive to the nuclear dynamics (in this case, solvent friction).

The observation ultimately of almost pure solvent dynamical control

(cobaltocene reactions; see figure) also allows approximate estimates of H_{if} to be obtained for the entire series of metallocenes.[107] The resulting H_{if} estimates, varying from about 0.075 to 1 kcal mol^{-1}, are in reasonable agreement with theoretical predictions by Newton and coworkers,[111,112] and can be understood qualitatively in terms of the primarily metal- and ligand-centered nature of the redox orbitals in the ferrocene and cobaltocene couples, respectively. The observation of clearly solvent-controlled adiabatic ET rates also enables the detailed nature of the solvation dynamics for activated ET processes to be explored. One aspect of this latter endeavor concerns the extent to which faster solvent dynamical components can accelerate the reaction rate beyond that prescribed by more overdamped motions. Comparisons between such kinetic data and subpicosecond TDFS measurements in non-Debye media (such as methanol) have demonstrated the importance of such effects.[108,109]

Prompted by theoretical work by Marcus and coworkers,[14,15] an important issue also receiving attention is the extent to which solvent dynamics can limit ET reaction rates even in the face of faster (and inherently underdamped) reactant vibrational components of the activation barrier. Experimental data has so far provided at least qualitative support to the theoretical predictions.[16,110]

Concluding Remarks

Although the foregoing is only an incomplete (and subjectively selective) survey of some experimental aspects of fundamental research in solution-phase ET processes, it is evident that much has been learned concerning the physical and

chemical factors that control activation energetics and dynamics, especially for small molecule reactions. In particular, the interplay between theory and experiment, initiated almost forty years ago by Marcus, is now stronger and more diverse than ever. This situation reflects not only the present buoyancy and health of the subject, but bodes well for the rapid development of our understanding of ET processes in much more complex systems. The future promises to be an exciting one!

Acknowledgments

The research at Northwestern and Purdue described in this article was supported in part by the Office of Naval Research.

Biographies

Joseph Hupp received a Ph.D. degree in chemistry in 1983 from Michigan State University where he studied with M. J. Weaver. After postdoctoral studies with T. J. Meyer at the University of North Carolina (1984-86) he joined the faculty at Northwestern University where he is currently a professor in the Department of Chemistry and a member of the Materials Research Center. His present interests include interfacial electrochemistry, photo-redox and mixed-valence chemistry, quantum confinement phenomena and mesoscopic chemistry, artificial molecular recognition effects, metallopolymer chemistry, and parenting of twins.

Michael Weaver received his Ph.D. in 1972 from Imperial College, London. Following postdoctoral research under Fred Anson at Caltech from 1972-75, he

was a faculty member at Michigan State University, moving to Purdue University in 1982, where he has been Professor of Chemistry since 1985. His current research interests span electrochemistry, electron-transfer chemistry, electrochemical applications of surface vibrational spectroscopies and scanning probe microscopies, and electrochemical surface science.

References

1. R.A. Marcus, J. Chem. Phys., 24, 966 (1956); 24, 979 (1956).
2. R.A. Marcus, Can. J. Chem., 37, 155 (1959).
3. R.A. Marcus Dis. Far. Soc., 29, 21 (1960).
4. R.A. Marcus, J. Phys. Chem., 67, 853 (1963).
5. R.A. Marcus, J. Chem. Phys., 43, 679 (1965).
6. R.A. Marcus. J. Phys. Chem., 72, 891 (1968).
7. J. Saveant, D. Tessier, Faraday Disc. Chem. Soc., 74, 57 (1982).
8. G.L. Closs and J.R. Miller, Science, 240, 440 (1987).
9. N. Sutin, Prog. Inorg. Chem., 30, 441 (1983).
10. R.A. Marcus, Int. J. Chem. Kinetics, 13, 865 (1981).
11. J.T. Hupp and M.J. Weaver, J. Electroanal. Chem., 152, 1 (1983).
12. M.J. Weaver, J. Phys. Chem., 94, 8608 (1990).
13. M.J. Weaver, Chem. Revs., 92, 463 (1992).
14. H. Sumi and R.A. Marcus, J. Chem. Phys., 84, 4894 (1986).
15. W. Nadler and R.A. Marcus, J. Chem. Phys., 86, 3906 (1987).
16. D.K. Phelps and M.J. Weaver, J. Phys. Chem., 96, 7187 (1992).
17. M.J. Powers and T.J. Meyer, J. Am. Chem. Soc., 98, 6731 (1976); 102, 1289 (1980).
18. R.W. Callahan and T.J. Meyer, Chem. Phys. Lett., 39, 82 (1976).
19. H. Taube, Pure Appl. Chem., 44, 25 (1975).
20. D.E. Richardson and H. Taube, J. Am. Chem. Soc., 105, 40 (1983).
21. D.O. Cowan and F. Kauffmann, J. Am. Chem. Soc., 92, 219 (1970).

22. C. Cruetz, Prog. Inorg. Chem., 30, 1 (1988).

23. R.A. Marcus, J. Chem. Phys., 43, 1261 (1965).

24. N.S. Hush, Trans. Faraday Soc., 57, 557 (1961).

25. J.T. Hupp, Y. Dong, R.L. Blackbourn, and H. Lu, J. Phys. Chem, 97, 3278 (1993).

26. G.M. Tom, C. Creutz, and H. Taube, J. Am. Chem. Soc., 96, 7828 (1974).

27. B.S. Brunschwig, S. Ehrenson, and N. Sutin, J. Phys. Chem., 90, 3657 (1986).

28. D.H. Oh, M. Sano, and S.G. Boxer, J. Am. Chem. Soc., 113, 6880 (1991).

29. G.M. Brown and N. Sutin, J. Am. Chem. Soc., 101, 883 (1979).

30. X.L. Zhang and J.T. Hupp, submitted for publication.

31. R. De La Rosa, P.S. Chang, F. Salaymeh, and J.C. Curtis, Inorg. Chem., 24, 4229 (1985).

32. K.S. Ennix, P.T. McMahon, and J.C. Curtis, Inorg. Chem., 26, 2660 (1987).

33. J.A. Roberts, J.C. Bebel, M.P. Absi, and J.T. Hupp, J. Am., Chem. Soc., 114, 7957 (1992).

34. Y. Dong, J.T. Hupp, and D.I. Yoon, J. Am. Chem. Soc., 115, 4379 (1993).

35. J.T. Hupp, J. Am. Chem. Soc., 112, 1563 (1990).

36. P.G. Wolynes, J. Am. Phys., 86, 5133 (1987); also see I. Rips, J. Klafter and J. Jortner, J. Chem. Phys., 88, 3246 (1988).

37. G.E. McManis, A. Gochev, R.M. Nielson, and M.J. Weaver, J. Phys. Chem., 93, 7733 (1989).

38. L. Blum and W.R. Fawcett, J. Phys. Chem., 96, 408 (1992).

39. W.R. Fawcett and M. Opallo, J. Phys. Chem., 96, 2920 (1992).

40. A.A. Kornyshev and J. Ulstrup, Chem. Phys. Lett., 126, 74 (1986).

41. D.K. Phelps, A.A. Kornyshev, and M.J. Weaver, J. Phys. Chem, 94, 1954 (1990).

42. R.A. Kuharski, J.S. Bader, D. Chandler, M. Sprik, M.L. Klein, and R.W. Impey, J. Chem. Phys., 89, 3248 (1988); J.S. Bader and D. Chandler, Chem. Phys. Lett., 157, 501 (1989).

43. T. Fonseca and B.M. Ladanyi, J. Phys. Chem., 95, 2116 (1991).

44. D.K. Phelps, M.J. Weaver, and B.M. Ladanyi, Chem. Phys., in press.

45. M.D. Todd, Y. Dong, and J.T. Hupp, Inorg. Chem., 30, 4605 (1991).

46. D.N. Hendrickson, S.M. Oh, T-Y. Dong, T. Kambara, M.J. Cohn and M.F. Moore, Comments Inorg. Chem., 4, 329 (1985).

47. J.T. Hupp and M.J. Weaver, J. Phys. Chem., 89, 1601 (1985).

48. R.A. Marcus, J. Phys. Chem., 94, 1050 (1990).

49. B.B. Smith and C.A. Koval, J. Electroanal. Chem., 227, 43 (1990).

50. See, for example: M. O'Neil, J. Marohn and G. McLendon, J. Am. Chem. Soc., 94, 4356 (1990).

51. B. O'Regan and M. Gratzel, Nature, 353, 737 (1991).

52. W. Pelouch, R. Ellingson, P. Powers, C.L. Tang, D.H. Levi, and A.J. Nozik, SPIE, 1677, 260 (1992).

53. R.A. Marcus, Trans. N.Y. Acad. Sci., 19, 423 (1957).

54. B.S. Brunschwig, C. Creutz, D.H. Macartney, T.-K. Sham, and N. Sutin, Faraday Discuss. Chem. Soc., 74, 113 (1982).

55. J.T. Hupp and M.J. Weaver, J. Phys. Chem., 89, 2795 (1985).

56. See, for example: E.M. Kober, J.V. Caspar, R.S. Lumpkin, and T.J. Meyer, J. Phys. Chem., 90, 3722 (1986).

57. See, for example, J.V. Caspar, T.D. Westmoreland, G.H. Allen, P.G. Bradley, T.J. Meyer, and W.H. Woodruff, J. Am. Chem. Soc., 106, 3492 (1984).

58. E.J. Heller, R.L. Sundberg, and D. Tannor, J. Phys. Chem., 86, 1822 (1982).

59. S.K. Doorn and J.T. Hupp, J. Am. Chem. Soc., 111, 1142 (1989).

60. S.K. Doorn and J.T. Hupp, J. Am. Chem. Soc., 111, 4704 (1989).

61. R.L. Blackbourn, C.S. Johnson, and J.T. Hupp, J. Am. Chem. Soc., 113, 1060 (1991).

62. R.L. Blackbourn, C.S. Johnson, J.T. Hupp, M.A. Bryant, R.L. Sobocinski, and J.E. Pemberton, J. Phys. Chem., 95, 10535 (1991).

63. F. Markel, N.S. Ferris, I.R. Gould, and A.B. Myers, J.Am. Chem. Soc., 114, 6208 (1992).

64. H. Lu, J. Prieskorn and J.T. Hupp, J. Am. Chem. Soc., 115, 4927 (1993).

65. V.I. Petrov, C.S. Mottley, J.T. Hupp, and L. Mann, submitted for publication.

66. M.D. Todd, A. Nitzan, and M.A. Ratner, J. Phys. Chem., 97, 29 (1993).

67. S.K. Doorn, P.O. Stoutland, R. Dyer, and W.H. Woodruff, J. Am. Chem. Soc., 114, 3133 (1993).

68. K.G. Spears and S. Arrivo, DOE Solar Photochemistry Research Conference Proceedings, NTIS, June 1993.

69. W. Jarzeba, K. Thakur, and P.F. Barbara, Chem. Phys., in press.

70. H.D. Abruna, B.M. Bommarito and D. Acevedo, Science, 250, 69 (1990).

71. M. Bedzyk and C.M. Mirkin, to be published.

72. J.V. Miller and J.V. Beitz, J. Chem. Phys., 71, 4579 (1979).

73. J. V. Miller, L.T. Calcaterra, and G.L. Closs, J. Am. Chem. Soc., 106, 3047

(1984).

74. W. Siebrand and D.F. Williams, J. Chem. Phys., 46, 403 (1967).

75. J.V. Caspar and T.J. Meyer, Chem. Phys. Lett., 91, 5 (1982).

76. R.A. Marcus, J. Phys. Chem., 90, 3460 (1986).

77. T.J. Meyer, Pure Appl. Chem., 58, 1193 (1986).

78. T.M. McCleskey, J.R. Winkler, and H.B. Gray, J. Am. Chem. Soc., 114, 6935 (1992).

79. G.L. McLendon, K. Pardue, and P. Bak, J. Am. Chem. Soc., 109, 7540 (1988).

80. J.M. Nocek, N. Liang, S.A. Wallin, A.G. Mauk, and B. Hoffman, J. Am. Chem. Soc., 112, 1623 (1990).

81. B.M. Hoffman and R.A. Ratner, J. Am. Chem. Soc., 109, 6237 (1987).

82. B.S. Brunschwig and N. Sutin, J. Am. Chem. Soc., 111, 7454 (1989).

83. D. Gust and T.A. Moore in "Advances in Photochemistry", Vol. 16, D.H. Volman, G.S. Hammond, and D.S. Neckers, eds., Wiley Interscience, New York, 1991, pp. 1-65.

84. R.A. Marcus, J. Phys. Chem., 72 891 (1968).

85. Representative work: D. Kim, I.S.H. Lee, and N.M. Kreevoy, J. Am. Chem. Soc., 112, 1889 (1990).

86. See, for example: A. Vassilian, H.A. Wishart, and S. Isied, J. Am. Chem. Soc., 112, 7278 (1990).

87. B.E. Bowler, A.L. Raphael, and H.B. Gray, Prog. Inorg. Chem., 38, 259 (1990).

88. C.E.D. Chidsey, C.R. Bertozzi, T.M. Putvinski, and A.M. Mujsce, A. Am. Chem. Soc., 112, 4301 (1990).

89. M.J. Weaver and T.T-T. Li, J. Phys. Chem., 90, 3823 (1986).

90. For example: J.T. Hynes, in "The Theory of Chemical Reactions", M. Baer, ed., Vol. 4, CRC Press, Boca Raton, FL, 1985, p. 171; J.T. Hynes, J. Stat. Phys., 42, 149 (1986); H. Frauenfelder and P.G. Wolynes, Science, 229, 337 (1985).

91. L.D. Zusman, Chem. Phys., 49, 295 (1980).

92. G. van der Zwan and J.T. Hynes, J. Chem. Phys., 76, 2993 (1982).

93. D.F. Calef and P.G. Wolynes, J. Phys. Chem., 87, 3387 (1983).

94. J.T. Hynes, J. Phys. Chem., 90, 3701 (1986).

95. H. Sumi and R.A. Marcus, J. Chem. Phys., 84, 4894 (1986); W. Nadler and R.A. Marcus, J. Chem. Phys., 86, 3906 (1987).

96. I. Rips and J. Jortner, J. Chem. Phys., 87, 2090 (1987).

97. M.D. Newton and H.L. Friedman, J. Chem. Phys., 88, 4460 (1988).

98. M. Sparpaglione and S. Mukamel, J. Phys. Chem., 91, 3938 (1987).

99. A. Chandra and B. Bagchi, Chem. Phys., 156, 323 (1991).

100. M. Maroncelli, J. MacInnis, and G.R. Fleming, Science, 243, 1674 (1989).

101. P.F. Barbara and W. Jarzeba, Adv. Photochem., 15, 1 (1990).

102. H. Heitele, Angew. Chem. Int. Ed. Eng., 32, 359 (1993).

103. But see: G. Grampp, M.C.B.L. Shohoji, B.J. Herold, and S. Steenken, Ber. Bunsenges Phys. Chem., 94, 1507 (1990); J.P. Telo, M.C.B.L. Shohoji, B.J. Herold, and G. Grampp, J. Chem. Soc. Far. Trans., 88, 47 (1992).

104. R.M. Nielsen, G.E. McManis, M.N. Golovin, and M.J. Weaver, J. Phys. Chem., 92, 3441 (1988); R.M. Nielsen, M.N. Golovin, G.E. McManis, and M.J. Weaver, J. Am. Chem. Soc., 110, 1745 (1988).

105. R.M. Nielsen, G.E. McManis, L.K. Safford, and M.J. Weaver, J. Phys.

Chem., 93, 2152 (1989).

106. R.M. Nielsen, G.E. McManis, and M.J. Weaver, J. Phys. Chem., 83, 4703 (1989).

107. G.E. McManis, R.M. Nielsen, A. Gochev, and M. J. Weaver, J. Am. Chem. Soc., 111, 5533 (1989).

108. M.J. Weaver, G.E. McManis, W. Jarzeba, and P.F. Barbara, J. Phys. Chem., 94, 1715 (1990).

109. M.J. Weaver and G.E. McManis, Acc. Chem. Res., 23, 294 (1990).

110. D.K. Phelps, M.T. Ramm, Y. Wang, S.F. Nelsen, and M.J. Weaver, J. Phys. Chem., 97, 181 (1993).

111. M.D. Newton, K. Ohta, and E. Zhang, J. Phys. Chem., 95, 2317 (1991).

112. M.D. Newton, Chem. Rev., 91, 767 (1991).

TABLE I

COMPARISON OF "SECOND-ORDER EQUIVALENT"
ELECTROREDUCTION RATES FOR SELECTED REACTIONS
AT MERCURY SURFACE WITH CORRESPONDING HOMOGENEOUS-PHASE RATES

Oxidant	Reductant	Solvent	k_1^e [a] $cm\ s^{-1}$	k_{12}^e [b] $M^{-1}\ s^{-1}$	k_{12}^h [c] $M^{-1}\ s^{-1}$
$Co(NH_3)_6^{3+}$	$Ru(NH_3)_6^{2+}$	H_2O	4×10^{-5}	1.3×10^3	0.45
$Ru(NH_3)_6^{3+}$	$Ru(NH_3)_6^{2+}$	H_2O	2.5	8.5×10^7	3.5×10^5
$Fe(OH_2)_6^{3+}$	$Ru(NH_3)_6^{2+}$	H_2O	- 5	$- 2 \times 10^8$	2.5×10^7
O_2	$Ru(NH_3)_6^{2+}$	H_2O	0.06	2×10^6	1.1×10^2
Cp_2Co^+	Cp_2Co	DMF	2.0	9×10^7	7×10^7
Cp_2Co^+	Cp_2Co	TMU	0.35	1.5×10^7	3.5×10^7

See ref. 12 for details.

a Work-corrected electrochemical rate constant for reduction of oxidant measured at formal potential of reductant redox couple.

b "Equivalent second-order" rate constant for electroduction, derived from k_1^e (see text and ref. 12).

c Second-order rate constant for homogeneous reaction.

Table II. Spectroscopic, Structural and Reorganizational Parameters for Electron Transfer from $Fe(CN)_6^{4-}$ to Colloidal TiO_2.

Mode	Relative Intensity	Δ^2	$\lvert\Delta a\rvert$	λ_i	Assignment
2118 cm^{-1}	20.0	0.95	0.048 Å	1000 cm^{-1}	ν_{C-N} bridge
2072	6.61	0.33	0.014	340	ν_{C-N} radial
2058	5.44	0.27	0.026	280	ν_{C-N} terminal
720	0.27	0.11	?	40	?
598	1.00	0.59	0.026*	180	ν_{Fe-C}
540	0.33	0.24	0.039	60	ν_{Fe-C} bridge
516	1.12	0.89	**	230	ν_{Ti-O}
484	0.90	0.82	**	200	ν_{Ti-O}
418	0.56	0.69	**	140	ν_{Ti-O}
364	0.27	0.43	0.059	80	ν_{Ti-N}

* Taken from (or taken as) the crystallographically determined value for $Fe(CN)_6^{4-/3-}$.

** Value not determined, since the measured normal coordinate displacement (Δ) may entail more than one type of bond length displacement (i.e., local-mode approximation may not be appropriate).

Figure Captions

Figure 1

Schematic representation of energy relationships for activated electron transfer.

Figure 2

Plot of E_{op} vs 1/d for the mixed-valence dimers $[(bpy)_2ClRu(L)RuCl(bpy)_2]^{3+}$, where L = pyrazine, 4,4'-bipyridine, *trans*-1,2-bis(4-pyridyl)ethylene (data from ref. 17).

Figure 3

Intervalence transfer band energies vs $1/\varepsilon_{op} - 1/\varepsilon_s$. Key to solvents: (1) nitrobenzene, (2) dimethyl sulfoxide, (3) 1-methyl-2-pyrrolidone, (4) hexamethylphosphoramide, (5) dimethylacetamide, (6) dimethylformamide, (7) formamide, (8) propylene carbonate, (9) acetone, (10) acetonitrile, and (11) deuterium oxide.

Figure 4

Log of k_s for the indicated ET reaction (eq. 13; normalized to k_s for $Ru(NH_3)_6^{3+/2+}$) versus the inverse radius of the reactant. The electrode material is low-defect-density HOPG; the electrolyte is 1 M aq. KCl. Line drawn is a best-fit line for all points except point 6 (open circle). Key to data points: (1) $Ru(NH_3)_6^{3+/2+}$, (2) $Ru(NH_3)_5(pyridine)^{3+/2+}$, (3) $(NH_3)_5Ru(pyrazine)Ru(NH_3)_5^{5+/4+}$, (4) $(NH_3)_5Ru(pyrazine)Ru(NH_3)_5^{6+/5+}$,(5) *t*-$(pyridine)(NH_3)_4Ru(pyrazine)Ru(NH_3)_4(pyrazine)^{5+/4+}$, (6) *t*-$(pyridine)(NH_3)_4Ru(pyrazine)\ Ru(NH_3)_4(pyrazine)^{6+/5+}$, and (7) $Fe(phenanthroline)_3^{3+/2+}$.

Figure 5

Plot of logarithm of work-corrected standard electrochemical rate constants k^o_{et} at mercury-aqueous interface versus calculated inner-shell activation barrier $\Delta G^{\ddagger}_{in}$. Data taken from J.T. Hupp and M.J. Weaver, Inorg. Chem, 22, 2557 (1983); T. Gennett and M.J. Weaver, Anal. Chem., 56, 1444 (1984).

Figure 6

Plot of log k_{ET} (s^{-1}) at colloidal TiO_2 versus reduction potentials (solution phase) for $Fe^{III}(CN)_5L^{n-}$ species.

Figure 7

Logarithmic plots of "barrier-corrected" rate constants (M^{-1} s^{-1}, extracted from rate and optical barrier data) versus inverse longitudinal relaxation time (s^{-1}) for five metallocene self-exchange reactions in 11 solvents, taken from ref. 29. See Table I of ref. 107 for key to solvents. Key to redox couples: filled circles, $Cp_2'Co^{+/0}$ (Cp' = pentamethylcyclopentadienyl); filled squares, $Cp_2^*Co^{+/0}$ [Cp^* = (carboxymethyl)cyclopentadienyl]; filled triangles, $Cp_2Co^{+/0}$; open triangles, $Cp_2Fe^{+/0}$; open squares, (hydroxylmethyl)ferrocenium/-ferrocene.

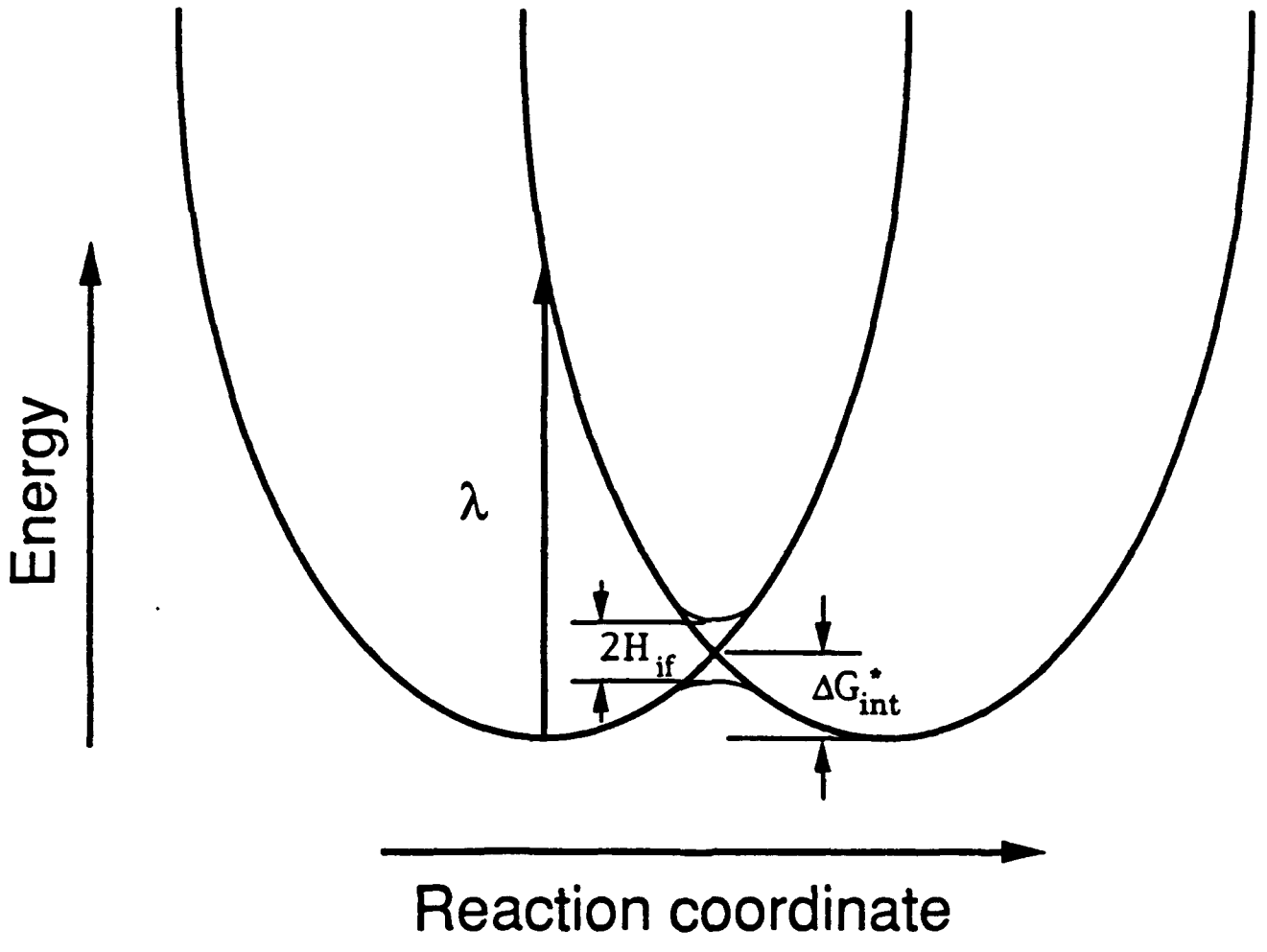

FIG 1

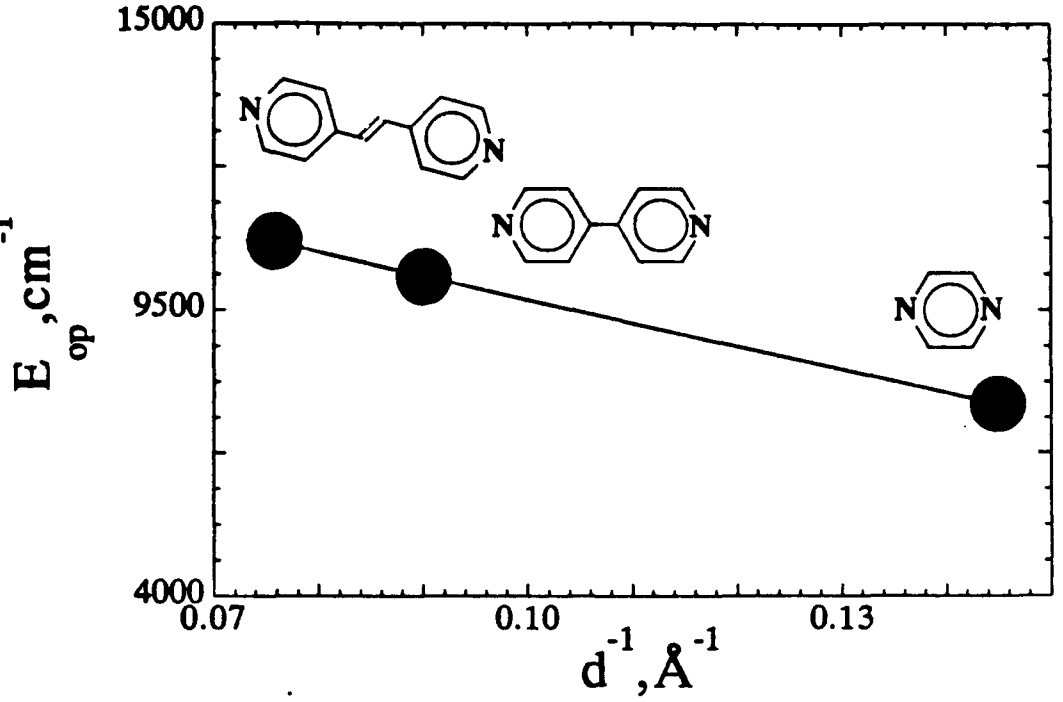
15000
9500
4000
0.07
0.10
0.13
E_{op} ,cm^{-1}
d^{-1} ,$Å^{-1}$
N
N
N
N
N
N

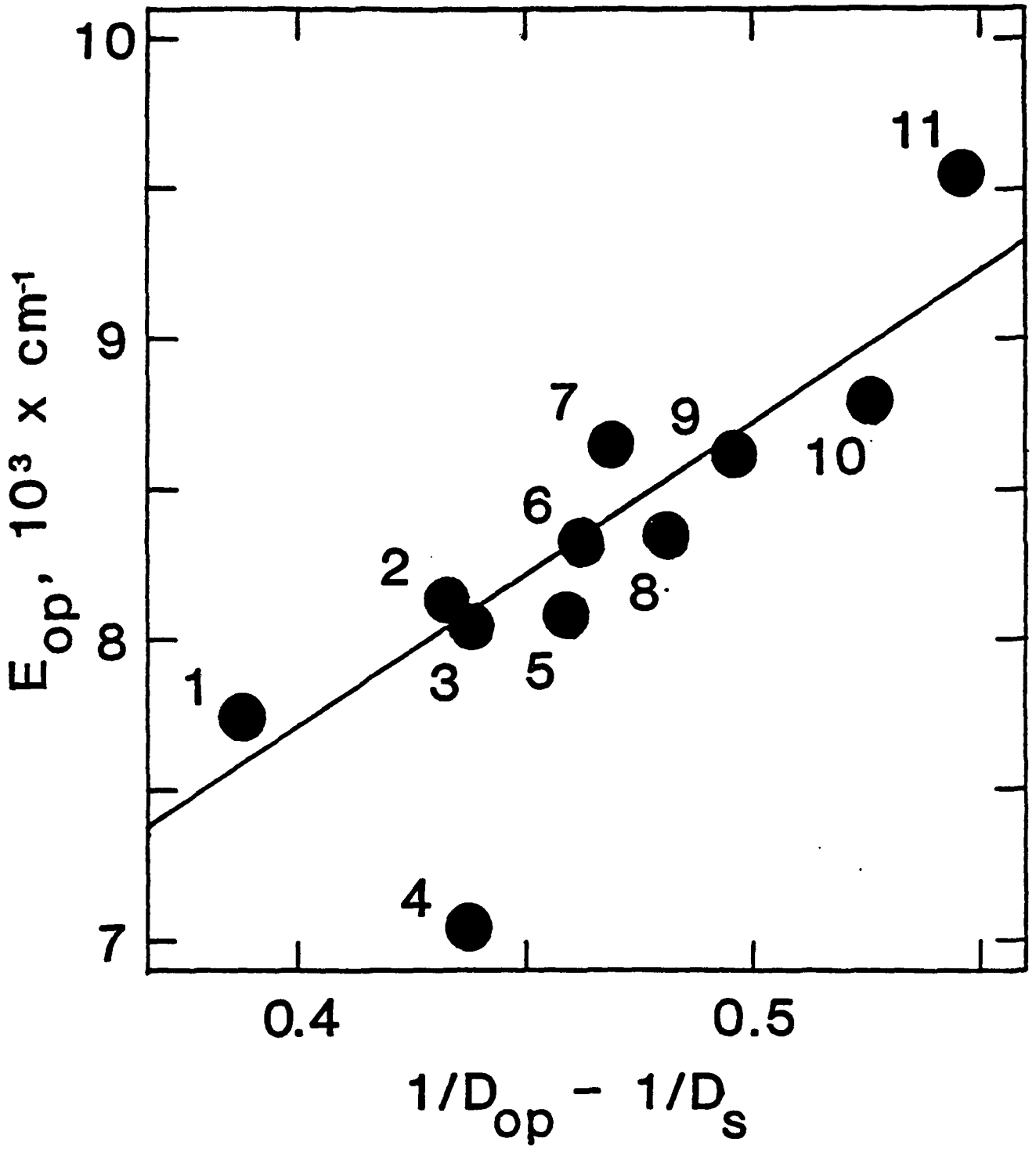
10
9
8
7
0.4
0.5
E_{op}, 10^3 x cm^{-1}
$1/D_{op} - 1/D_s$
1
2
3
4
5
6
7
8
9
10
11

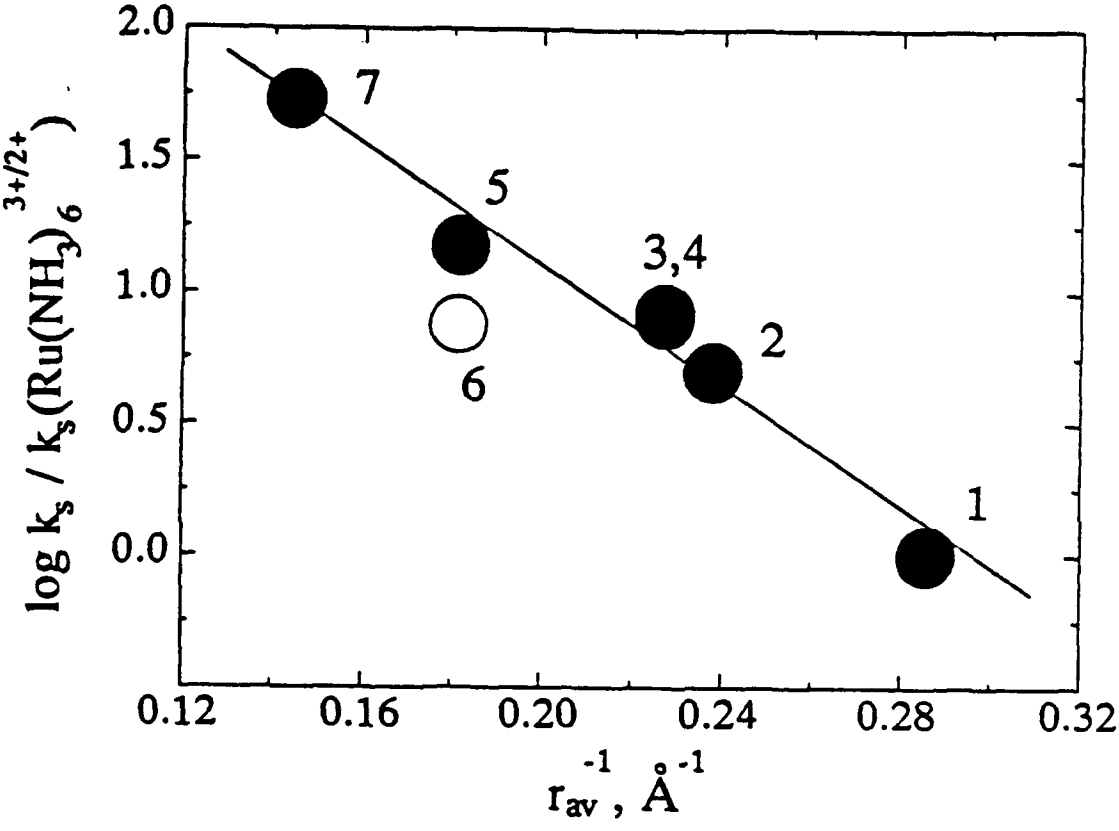
2.0
1.5
1.0
0.5
0.0
log k_s / $k_s(Ru(NH_3)_6^{3+/2+})$
7
5
3,4
2
6
1
0.12
0.16
0.20
0.24
0.28
0.32
r_{av}^{-1} , Å^{-1}

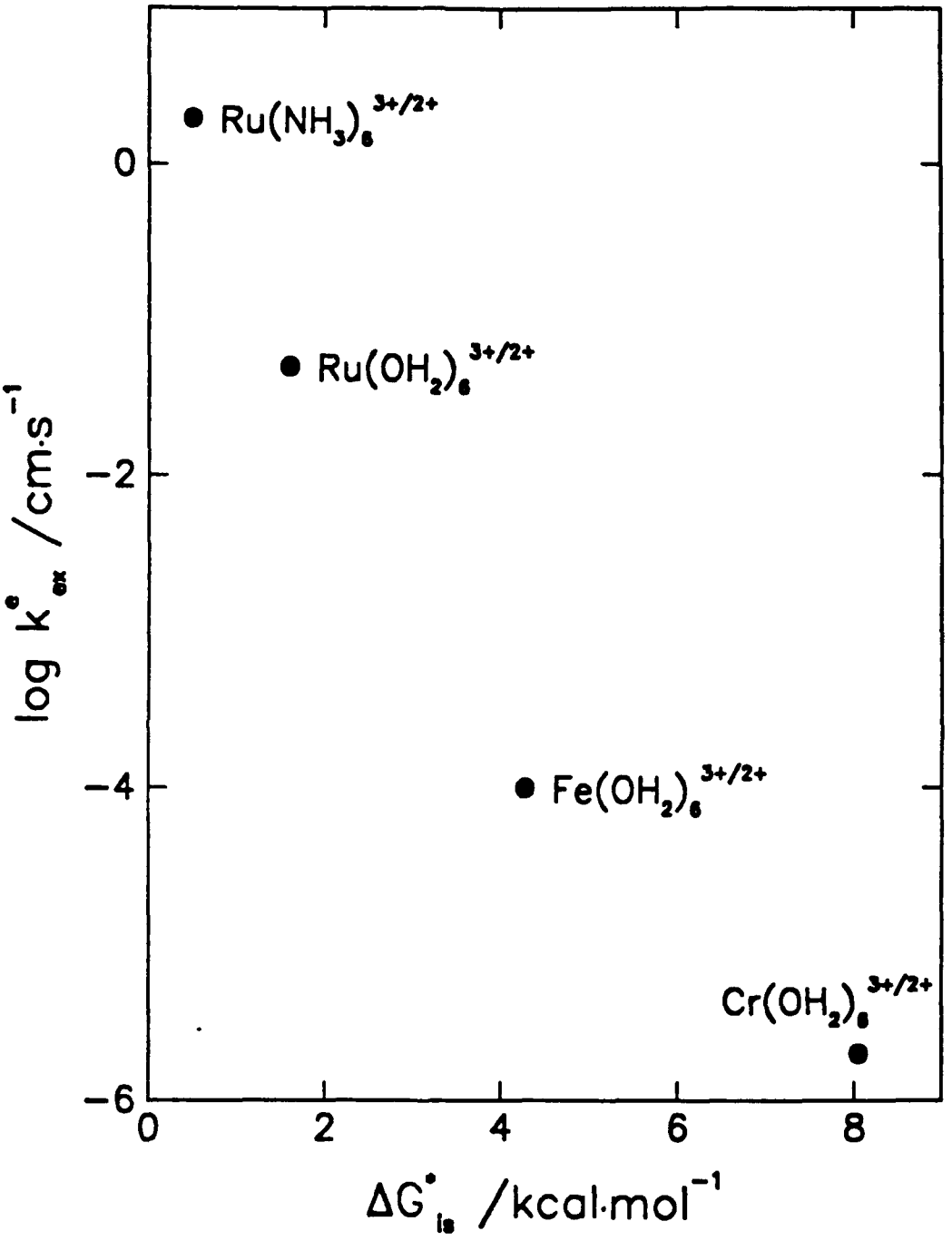
Ru(NH3)6 3+/2+
Ru(OH2)6 3+/2+
Fe(OH2)6 3+/2+
Cr(OH2)6 3+/2+
0
−2
−4
−6
0
2
4
6
8
log k°ex /cm·s−1
ΔG°is /kcal·mol−1

F 6 5

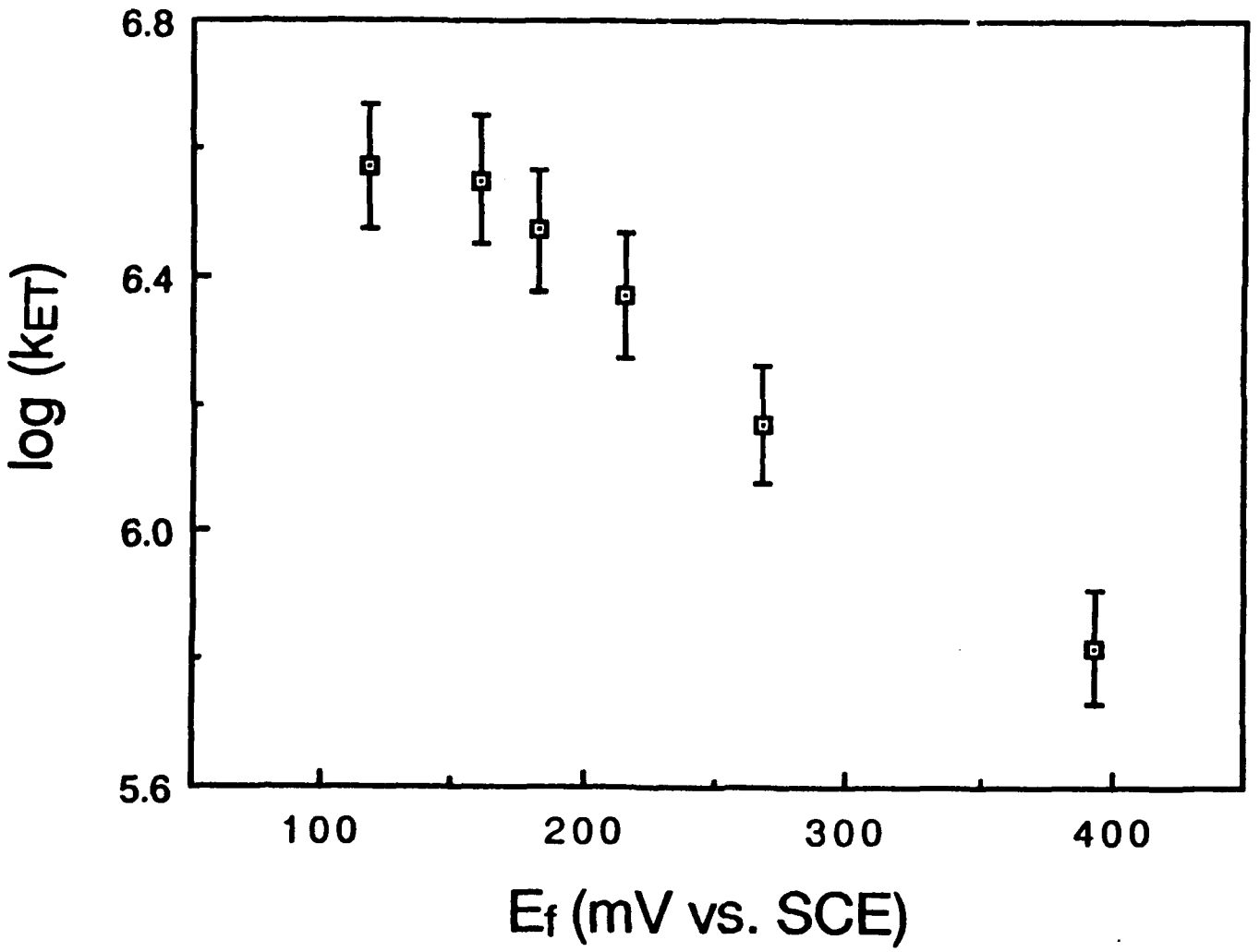
6.8
6.4
6.0
5.6
log (k_{ET})
100
200
300
400
E_f (mV vs. SCE)

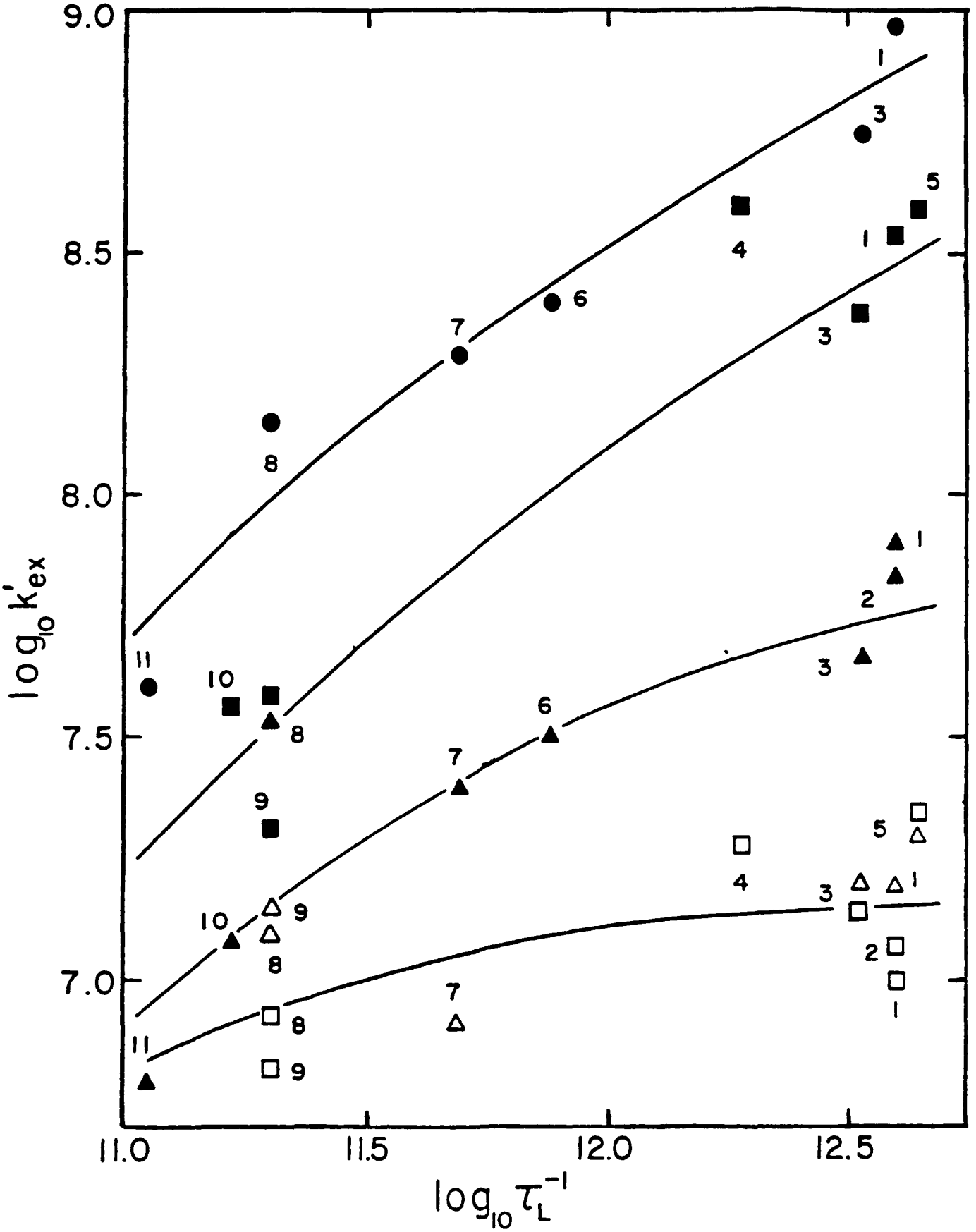

FIG 7